

Advanced MRI findings in patients with breast hamartomas

Gülner Erdem, Hakkı Muammer Karakaş, Burak Işık, Ahmet Kemal Fırat

PURPOSE

Although it has been stated that breast hamartomas are rare tumors, radiologists frequently encounter them in their daily practices. Fat, glandular and fibrous tissues all produce a mass of disorganized but mature specialized cells. Because hamartomas do not have specific diagnostic histological features, the clinical and radiological findings are important in their diagnosis. The aim of this study is to present the advanced magnetic resonance imaging (MRI) findings of breast hamartomas.

MATERIALS AND METHODS

Eight patients with breast hamartomas were examined using MRI techniques in addition to ultrasonographic and/or mammographic findings.

RESULTS

Each of the lesions examined showed a gradual enhancement pattern in its time-signal intensity curve on dynamic contrast-enhanced MRI. On MR spectroscopy, water and lipid peaks were detected that resembled normal breast tissue. The diffusion features of the lesions were variable due to the different ratios of the tissue elements constituting them on diffusion-weighted imaging (DWI).

CONCLUSION

Advanced MRI findings may clarify diagnoses by providing additional information following sonography, especially in lactating or pregnant women, in whom mammographic examination is not preferred.

Key words: • breast • hamartoma • magnetic resonance imaging • diffusion magnetic resonance imaging • magnetic resonance spectroscopy

Although classical textbooks state that hamartomas are rare tumors, radiologists who use both mammography and ultrasonography (US) frequently encounter hamartomas in their daily practices. These tumors present as painless and mobile masses with well-defined borders. They are composed of variable amounts of glandular tissue, fat and fibrous elements that produce a mass of disorganized but mature specialized cells or tissues (1–3). The complete resemblance of the tissues to normal breast parenchyma and an occasional admixture of other elements limit the contribution of the pathological examination to the diagnosis. The correlation between clinical and radiological findings is of paramount importance (4, 5). Although mammographic and US findings of breast hamartomas have been well defined, advanced magnetic resonance imaging (MRI) findings in such cases have not been previously described. This study provides a description of dynamic contrast-enhanced MRI (DCE-MRI), diffusion-weighted imaging (DWI) and MR spectroscopy (MRS) findings in breast hamartomas.

Materials and methods

The study was executed retrospectively based on the records of our breast imaging center over a 24-month period. During that time, all examinations were performed by the same radiologist (G.E.), who is a specialist in breast imaging. Eight patients with a diagnosis of breast hamartoma were found in the center's registry. The ages of these patients ranged from 22 to 54 years (mean age, 38.6 years; SD, 14.6 years). These patients were initially examined with US and/or mammography either as part of a routine screening or as a work-up for palpable breast masses. Cases in which the masses were diagnosed as hamartomas were further examined via MRI. These patients each underwent an MRI examination to reveal advanced imaging characteristics of these rare lesions as part of an institutional research study on DCE-MRI, DWI and MRS. Informed consent was obtained from all patients. MRI scans were conducted using a 1.5 T scanner (Intera Master, Gyroscan, Philips, The Netherlands) with a gradient force of 32 mT/m. Images were obtained in the prone position using a standard breast coil.

Axial and sagittal T1-weighted (TR/TE, 550/11 ms), T2-weighted (TR/TE, 2429/120 ms), and fat-suppressed T1-weighted images were obtained for conventional MRI examinations. DCE-MRI was performed after intravenous administration of 0.1 mmol/kg gadopentetate dimeglumine (Gd-DTPA) with an automatic injector (Spectris, Medrad, USA). In this study, 12 consecutive T1-weighted fast field echo (FFE) sequences, each lasting 20 seconds, were obtained in four minutes. After subtracting the initial unenhanced images from the remaining enhanced images, the regions of interest (ROIs) were placed on the most enhancing area within the mass. Time intensity curves (TICs) were constructed to quantitative-

From the Departments of Radiology (G.E. ✉ gerdem@inonu.edu.tr, H.M.K., A.K.F.), and General Surgery (B.I.), İnönü University School of Medicine, Malatya, Turkey.

Received 29 September 2009; revision requested 19 October 2009; revision received 27 October 2009; accepted 7 December 2009.

Published online 26 July 2010
DOI 10.4261/1305-3825.DIR.1892-08.2

ly show time-dependent enhancement in these ROIs.

For DWI, a single-shot gradient-echo echo-planar imaging (EPI) sequence (TR/TE, 4393/81 ms; slice thickness, 5 mm; interslice gap, 1 mm; FOV, 350 mm; matrix, 128x256) was used. Diffusion gradients were simultaneously applied to the x, y and z axes. "b" values of 0 and 1000 s/mm² were used to construct automated apparent diffusion coefficient (ADC) maps using commercially available software. Directionally averaged ADC values were measured on ADC maps to quantify the diffusional properties of the masses. Measurements were performed using circular ROIs drawn onto the regions identified on the T2-weighted (b=0 s/mm²) images. These ROIs were 150 to 850 mm² in area, depending on the size of the mass. The sizes of the control ROIs were determined such that they matched the size of the relevant mass. All measurements were performed three times, and the averages of these measurements were calculated and used for the final analysis.

The Statistical Package for Social Sciences version 13.0 (SPSS Inc., Chicago, USA) was used for the statistical analysis. Results were given as means±standard deviations (SD). Mann-Whitney U test was utilized for comparison of the ADC values between the lesions and normal breast tissues.

MRS of each mass was performed by the point-resolved spectroscopy technique with a short (31 ms) and long (136 ms) TE. The ROI for MRS measurement was placed at the center of the mass to avoid a contamination signal from normal tissues. The spectra were generated and corrected with the scanner's own software.

Results

The mean age of presentation or incidental discovery was 38.6 years in our patients. Two out of three patients who were under that mean age (22 and 26 years) were lactating. Although these patients had noticed some breast lumps since pubertal ages, these masses had undergone a considerable change in size after they gave birth. These patients were initially investigated with US in non-specialized medical institutions upon self-palpation of painless masses. Although the US features of these masses resembled fibroadenomas, they were slightly heterogene-

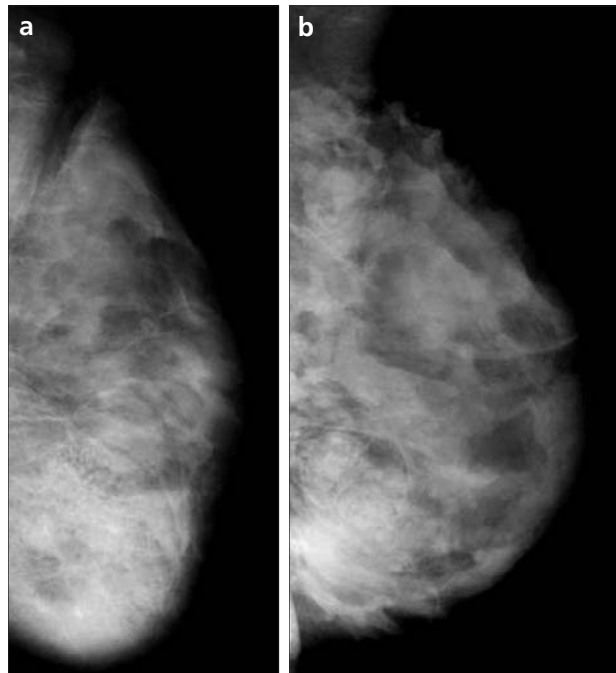


Figure 1. a, b. Mammographies (mediolateral oblique views) of two different patients. A large well-defined, oval opacity with a mixed density at the lower region of the right breast is seen in a 22-year-old lactating woman (a). A heterogeneous opacity surrounded by a thin radiopaque pseudocapsule at the lower region of the left breast is present in a 26-year-old lactating woman (b).

ous. Therefore, the two patients were referred to our institution for detailed work-ups. Taking their age group into account, their conventional mammographic examinations were limited to a single position.

Two patients presented with premenstrual pain. One of these patients and the remainder of the study group were discovered during routine mammographic screenings. Three of these patients were postmenopausal.

All lesions were solitary, with maximum diameters between 2.5 and 10.0 cm (mean, 5.3 cm; SD 2.6 cm). All of the patients were investigated with mammography except for one young patient who had dense pattern on US. Six of these had mammographically detectable lesions that were ovoid in shape and had well-defined, thin capsules with heterogeneous parenchymal patterns. The presence of widely dispersed fat densities was their main radiological hallmark (Fig. 1). US examination of these patients revealed ovoid masses with well-defined contours, the echogenic features of which were similar to fibroadenomas. However, compared to fibroadenomas, the echogenicity of the masses was slightly higher and heterogeneous, and their posterior acoustic enhancement was either nonexistent or less prominent (Fig. 2).

On conventional T1- and T2-weighted MRI, these lesions had heterogene-

ous intensities that represented their fatty and fibroglandular content, as well as a thin capsule (Fig. 3). On DCE-MRI the lesions enhanced gradually. This enhancement was classified as a type 1 pattern (Fig. 4). On DWI, a distinct signal pattern was not present. The mean ADC value of the lesions was $1147\pm383\times10^{-6}$ mm²/s, whereas the value of the normal breast parenchyma was $986\pm352\times10^{-6}$ mm²/s.

The difference in ADC values between hamartomas and normal breast parenchyma was not significant (Mann-Whitney U test, $P = 0.345$). The ADCs of hamartomas and normal parenchyma are given in Table.

On MRS, short (31 ms) and long (136 ms) TE spectra exhibited lipid peaks. These peaks are indicative of benign lesions. Choline peak, a malignancy marker that represents cell membrane turnover, was not present (Fig. 5).

Five of these patients were investigated with fine needle aspiration cytology by the request of their clinicians. The pathological evaluations of these specimens were reported as purely benign without any atypical cells.

Discussion

Breast hamartomas are benign lesions that appear with a frequency of 0.1–0.7% within all benign mammary masses (4). These lesions are also called fibroadenolipomas, lipofibroadenomas and adenolipomas. As these

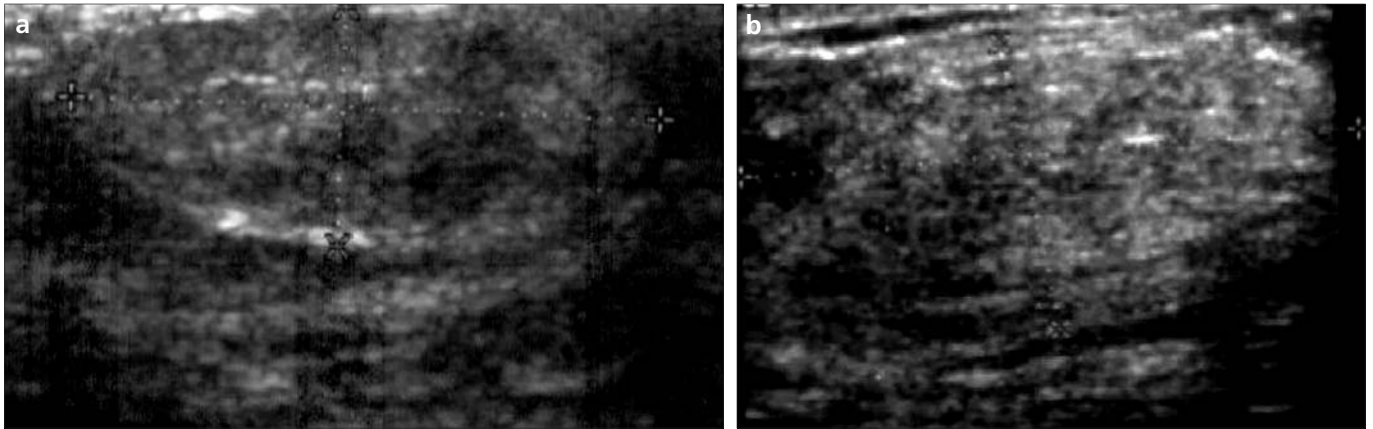


Figure 2. a, b. Ultrasonographic appearances of two different hamartoma cases. Isoechoic oval masses with hypoechoic areas representing fat tissues are seen without posterior acoustic enhancement in a 22-year-old woman (a) and a 47-year-old woman (b) who both presented with premenstrual pain.

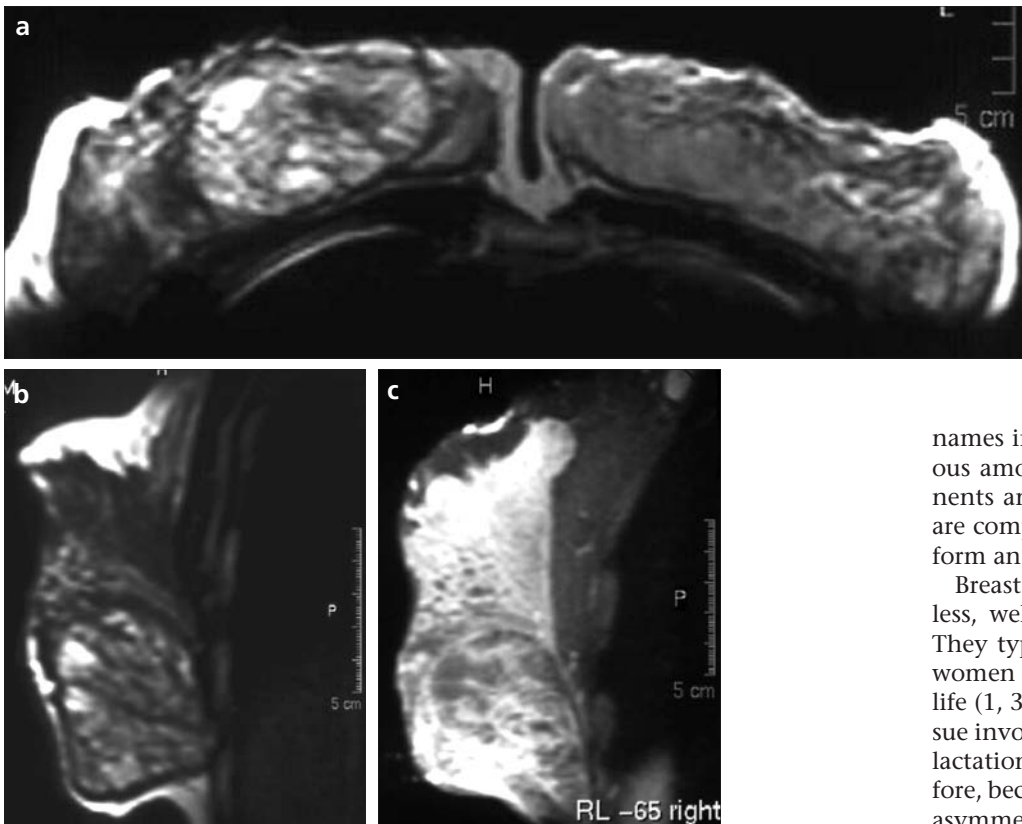


Figure 3. a–c. Axial (a) and sagittal (b) T2-weighted MR images. A heterogeneous hyperintense mass with well-defined margins and a smooth hypointense rim at the lower region of the right breast was found in a 22-year-old lactating woman. On sagittal post-contrast T1-weighted fat-suppressed MR image (c), the mass containing fat intensities enhances heterogeneously.

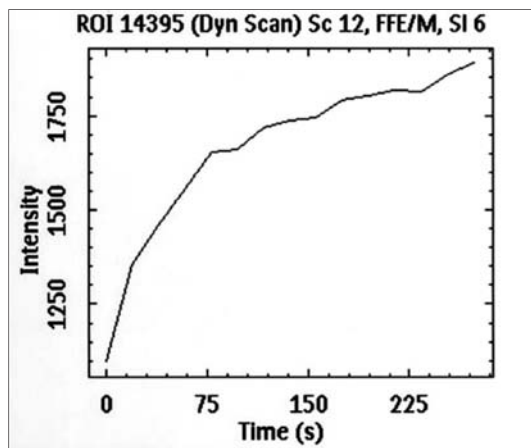


Figure 4. The time-signal intensity curve obtained from dynamic contrast enhanced MRI demonstrates the presence of a gradual enhancement pattern in favor of a benign lesion.

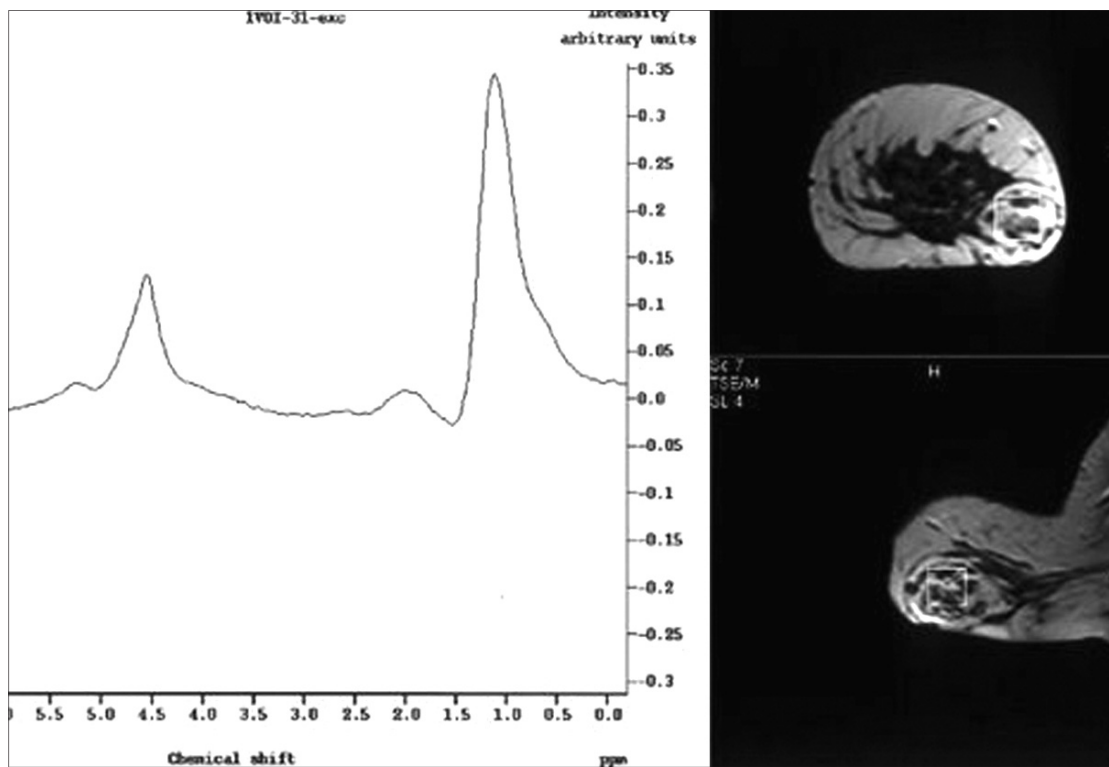
names imply, the lesions contain various amounts of fat, glandular components and fibrous tissue. These tissues are completely differentiated, but they form an abnormal organization (1–3).

Breast hamartomas constitute painless, well-defined and mobile masses. They typically present in middle-aged women during the 4th–5th decades of life (1, 3). During these ages, breast tissue involutes as a consequence of post-lactation or menopause. Lesions, therefore, become more apparent, leading to asymmetric enlargement (6). Estrogen and progesterone receptor positivity in such lesions were shown to be similar to normal breast tissue in immunohistochemical studies. Ki67 together with receptor positivity may reflect some proliferative activity and explain the observed faster growth of hamartomas during pregnancy and lactation (7). These tumors are frequently unilateral (8) and may develop in ectopic breast tissue in the inguinal or axillary regions (9, 10).

The mammographic appearance of a hamartoma is fairly characteristic; it is referred to as a “breast-in-breast” lesion and is observed as a well-defined mass.

Table. Patient demographic data, and mean ADC values of hamartomas and normal breast parenchyma

Age (years)	Complaint	Size (cm)	Mean ADC values of hamartomas (mm ² /s x10 ⁻⁶)	Mean ADC values of normal breast parenchyma (mm ² /s x10 ⁻⁶)
22	Palpable mass during lactation	10	1120	826
26	Palpable mass during lactation	4	1396	1387
22	Premenstrual pain	2.5	1071	1407
47	Premenstrual pain	7	1724	1188
46	Screening	4	1001	690
53	Screening	3.5	1176	1056
54	Screening	3.7	1301	959
54	Screening	8	386	378

**Figure 5.** MR spectroscopic analysis. Elevated lipid signals at 1.1 ppm and water signals at 4.5 ppm were observed on short TE (31 ms).

The shape of the mass is round to oval, and it has a mixed density composed of a mixture of fatty and fibroglandular tissues. The mass is surrounded by a thin radiopaque pseudocapsule, and the degree of opacity depends on the constituents of the hamartomatous tissue (1–4). The lobulated densities scattered within the encapsulated fat are called “slices of salami”. These densities may be accompanied by benign amorphous or round microcalcifications. The mass may replace the subcutaneous fatty tissue without altering the skin (2).

The above-mentioned mammographic findings may be adequate for

diagnosing hamartomas, bypassing the need for advanced examinations such as US or biopsy (2). However, these mammographic findings are present in relatively bigger lesions, and is seen in 10–60% of hamartomas (1). On US, a lesion with a heterogeneous internal echo pattern that is composed of echogenic fibrous and hypoechoic components is observed (4). This lesion may also be isoechoic and contain cystic areas. The role of ultrasonography in diagnosis is limited due to the variety of possible US appearances (1, 3). MRI of hamartomas reveals internal fat intensities in addition to heterogeneous contrast enhancement and re-

veals a smooth, thin hypointense rim (4). While heterogeneous masses containing radiolucent areas with thin, opaque capsules were seen in six of our patients using mammography, the lesion could not be discriminated due to the underlying density of the breast tissue in one case. All hamartomas were observed as well-defined masses that were isoechoic or had mixed echogenicity within small cystic areas on US. On MRI, all but one case had well-defined, heterogeneously intense lesions.

The presence of lobules and ducts differentiates hamartomas from fibroadenomas (11). However, hamartomas do not have specific diagnostic

histological findings (4, 5). Fine needle aspiration biopsy and core biopsy have limited roles in the diagnosis of hamartomas; therefore, the diagnosis of hamartomas may be fairly difficult. The clinical and radiological findings are important. Although they are benign, there is always a possibility of recurrence. Moreover, these lesions may coexist with in situ or invasive carcinomas (4, 12, 13). The malignancy itself may arise from glandular parts of hamartomatous tissues (13). Given the above-mentioned situations, conventional and functional MRI are clear complements to mammographic and ultrasonographic studies. These advanced methods also constitute the most appropriate imaging modalities in pregnant and lactating women.

Although the diagnosis of breast lesions essentially depends on mammographic and US findings, MRI features have increasingly been reported. These reports are focused on enhancement patterns and biochemical features that would allow the differentiation between benign and malignant lesions. DCE-MRI gives information on the vascularization of tissues. Peak enhancement in the early phases and rapid washout demonstrate increased vascularization and are malignancy criteria (14). In all of our cases, lesions showed gradual enhancement patterns in their time-intensity curves, indicative of benign lesions.

MRS is one of the most advanced functional imaging modalities. It provides information about the biochemical structure and metabolism of tissues. The level of different chemical metabolites may be measured by this method. The presence of choline peaks is a diagnostic metabolic marker in malignant breast tumors. Choline is observed at 3.24 ppm in the spectrum and is not seen in benign lesions (15). In MRS, we

detected marked water and lipid peaks; however, choline peaks were not detected. These results are similar to the signals seen in normal breast tissue.

DWI allows quantitative measurement of the diffusion motion of the water molecules in lesions and normal tissues, and ADC mapping shows the absolute value of diffusion. The mean ADC value of lesions in this study ($1147 \pm 383 \times 10^{-6} \text{ mm}^2/\text{s}$) was similar to that of normal breast parenchyma ($986 \pm 352 \times 10^{-6} \text{ mm}^2/\text{s}$). There was no significant difference between the groups. We considered that different values among the cases may have resulted from the different ratios of the tissue elements constituting the lesions. The ADC value may be higher in lesions where fat and glandular elements are dominant, whereas the value may be lower in lesions where fibrous elements are dominant (16).

In conclusion, breast hamartomas are rare breast masses, and in order to reach the correct diagnosis in these cases, a correlation between the clinical and radiological findings is required due to the inadequacy of pathological examinations alone. The diagnosis of breast lesions depends on mammographic and US findings. However, especially in lactating or pregnant women, in whom mammographic examinations are not preferred, the conventional and advanced MRI findings could clarify the diagnosis by providing additional information following US.

References

1. Pui MH, Movson IJ. Fatty tissue breast lesions. *Clin Imaging* 2003; 27:150–155.
2. Muttarak M, Chaiwu B. Imaging of giant breast masses with pathological correlation. *Singapore Med J* 2004; 45:132.
3. Sanal HT, Ersöz N, Altinel Ö, Ünal E, Can C. Giant hamartoma of the breast. *Breast J* 2006; 12:84–85.

4. Tse GMK, Law BKB, Ma TKF, et al. Hamartoma of the breast: a clinicopathological review. *J Clin Pathol* 2002; 55:951–954.
5. Hattori H. Mammary hamartoma of the axillary subcutis. *Breast J* 2006; 12:181–182.
6. Scott-Conner CE, Powers C, Subramony D, Didlake RH. Changing clinical picture of mammary hamartoma. *Am J Surg* 1993; 165:208–212.
7. Herbert M, Sandbank J, Liokumovich P, et al. Breast hamartomas: clinicopathological and immunohistochemical studies of 24 cases. *Histopathology* 2002; 41:30–34.
8. Kuroda N, Goishi K, Ohara M, Hirouchi T, Mizumo K, Nakagawa K. Bilateral hamartoma arising in axillary accessory mammary glands. *APMIS* 2006; 114:77–78.
9. Reck T, Dworak O, Thaler KH, Kockerling F. Hamartoma of aberrant breast tissue in the inguinal region. *Chirurg* 1995; 66:923–926.
10. da Silva BB, Rodrigues JS, Borges US, Pires CG, Pereira da Silva RF. Large mammary hamartoma of axillary supernumerary breast tissue. *Breast* 2006; 15:135–136.
11. Daya D, Trus T, D'Souza TJ, Minuk T, Yemen B. Hamartoma of the breast, an underrecognized breast lesion. A clinicopathologic and radiographic study of 25 cases. *Am J Clin Pathol* 1995; 103:685–689.
12. Ruiz Tovar J, Reguero Callejas ME, Alaez AB, et al. Infiltrating ductal carcinoma and ductal carcinoma in situ associated with mammary hamartoma. *Breast J* 2006; 12:368–370.
13. Anani PA, Hessler C. Breast hamartoma with invasive ductal carcinoma. Report of two cases and review of the literature. *Pathol Res Pract* 1996; 192:1187–1194.
14. Tunçbilek N, Karakaş HM, Ökten OO. Dynamic magnetic resonance imaging in determining histopathological prognostic factors of invasive breast cancers. *Eur J Radiol* 2005; 53:199–205.
15. Kim JK, Park SH, Lee HM, et al. In vivo ^1H -MRS evaluation of malignant and benign breast disease. *Breast* 2003; 12:179–182.
16. Kinoshita T, Yashiro N, Ihara N, Funatu H, Fukuma E, Narita M. Diffusion-weighted half-fourier single-shot turbo spin echo imaging in breast tumors: differentiation of invasive ductal carcinoma from fibroadenoma. *J Comput Assist Tomogr* 2002; 26:1042–1046.